Neuropharmacology 105 (2016) 577–586

Contents lists available at ScienceDirect

Neuropharmacology

journal homepage: www.elsevier.com/locate/neuropharm

Stress induces analgesia via orexin 1 receptor-initiated endocannabinoid/CB1 signaling in the mouse periaqueductal gray

Hsin-Jung Lee [a], Lu-Yang Chang [b], Yu-Cheng Ho [b], Shu-Fang Teng [a], Ling-Ling Hwang [d], Ken Mackie [e], Lih-Chu Chiou [a, b, c, f, *]

[a] Department of Pharmacology, College of Medicine, National Taiwan University, Taipei, Taiwan
[b] Graduate Institute of Pharmacology, College of Medicine, National Taiwan University, Taipei, Taiwan
[c] Graduate Institute of Brain and Mind Sciences, College of Medicine, National Taiwan University, Taipei, Taiwan
[d] Department of Physiology, Taipei Medical University, Taipei, Taiwan
[e] Gill Center and the Department of Psychological and Brain Sciences, Indiana University, Bloomington, IN, USA
[f] Research Center for Chinese Medicine & Acupuncture, China Medical University, Taichung, Taiwan

ARTICLE INFO

Article history:
Received 7 December 2015
Received in revised form
1 February 2016
Accepted 15 February 2016
Available online 18 February 2016

Chemical Compounds:
AM 251 (PubChem CID: 2125)
morphine (PubChem CID: 5464110)
naloxone (PubChem CID: 5464092)
naltrexone (PubChem CID: 5485201)
SB 334867 (PubChem CID: 6604926)
TCS-OX2–29 (PubChem CID: 53302033)
WIN 55,212-2 (PubChem CID: 5311501)

Keywords:
Orexin
OX1 and OX2 receptors
Pain
Cannabinoid
Stress-induced analgesia
Periaqueductal gray

ABSTRACT

The orexin system consists of orexin A/hypocretin 1 and orexin B/hypocretin 2, and OX1 and OX2 receptors. Our previous electrophysiological study showed that orexin A in the rat ventrolateral periaqueductal gray (vlPAG) induced antinociception via an OX1 receptor-initiated and endocannabinoid-mediated disinhibition mechanism. Here, we further characterized antinociceptive effects of orexins in the mouse vlPAG and investigated whether this mechanism in the vlPAG can contribute to stress-induced analgesia (SIA) in mice. Intra-vlPAG (*i.pag.*) microinjection of orexin A in the mouse vlPAG increased the hot-plate latency. This effect was mimicked by *i.pag.* injection of WIN 55,212-2, a CB1 agonist, and antagonized by *i.pag.* injection of the antagonist of OX1 (SB 334867) or CB1 (AM 251), but not OX2 (TCS-OX2-29) or opioid (naloxone), receptors. [Ala[11], D-Leu[15]]-orexin B (*i.pag.*), an OX2 selective agonist, also induced antinociception in a manner blocked by *i.pag.* injection of TCS-OX2-29, but not SB 334867 or AM 251. Mice receiving restraint stress for 30 min showed significantly longer hot-plate latency, more c-Fos-expressing orexin neurons in the lateral hypothalamus and higher orexin levels in the vlPAG than unrestrained mice. Restraint SIA in mice was prevented by *i.pag.* or intraperitoneal injection of SB 334867 or AM 251, but not TCS-OX2-29 or naloxone. These results suggest that during stress, hypothalamic orexin neurons are activated, releasing orexins into the vlPAG to induce analgesia, possibly via the OX1 receptor-initiated, endocannabinoid-mediated disinhibition mechanism previously reported. Although activating either OX1 or OX2 receptors in the vlPAG can lead to antinociception, only OX1 receptor-initiated antinociception is endocannabinoid-dependent.

1. Introduction

Orexin A and orexin B (Sakurai et al., 1998), also known as hypocretin 1 and hypocretin 2 (de Lecea et al., 1998), are two hypothalamic neuropeptides derived from a precursor protein, prepro-hypocretin. Two orexin receptors, OX1 and OX2, have been identified. OX1 and OX2 receptors are Gq-protein coupled receptors (GqPCRs), with OX2 receptors also coupling to additional G-protein pathways (Tsujino and Sakurai, 2009). OX1 and OX2 receptors display similar affinity for orexin A while OX2 receptors have higher affinity for orexin B (Sakurai et al., 1998). Orexin-containing neurons are uniquely localized in the lateral and perifornical area of the hypothalamus (de Lecea et al., 1998; Sakurai et al., 1998), but send

Abbreviations: 2-AG, 2-arachidonoylglycerol; AL-orexin B, [Ala[11], D-Leu[15]] orexin-B; AM 251, 1-(2,4-dichlorophenyl)-5-(4-iodophenyl)-4-methyl-N-1-piperidinyl-1H-pyrazole-3-carboxamide; AUC, area under the curve; CB1 receptor, cannabinoid 1 receptor; TCS-OX2-29, (2S)-1-(3,4-dihydro-6,7-dimethoxy-2(1H)-isoquinolinyl)-3,3-dimethyl-2-[(4-pyridinylmethyl)amino]-1-butanone hydrochloride; DAG, diacylglycerol; DAGL, diacylglycerol lipase; GqPCR, Gq-protein coupled receptor; *i.pag.*, intra-vlPAG microinjection; MPE, maximal possible effect; OX1 receptor, orexin 1 receptor; OX2 receptor, orexin 2 receptor; PLC, phospholipase C; SB 334867, 1-(2-Methyylbenzoxanzol-6-yl)-3-[1,5]naphthyridin-4-yl-urea hydrochloride; SIA, stress-induced analgesia; vlPAG, ventrolateral periaqueductal gray; WIN 55,212-2, *R*)-(+)-[2,3-Dihydro-5-methyl-3-(4-morpholinylmethyl)pyrrolo [1,2,3-*de*]-1,4-benzoxazin-6-yl]-1-naphthalenylmethanone mesylate.

* Corresponding author. Department of Pharmacology, College of Medicine, National Taiwan University, No. 1, Jen-Ai Rd., Section 1, Taipei, 100, Taiwan.
E-mail address: lcchiou@ntu.edu.tw (L.-C. Chiou).

http://dx.doi.org/10.1016/j.neuropharm.2016.02.018
0028-3908/

projections widely throughout the brain and spinal cord (Peyron et al., 1998; van den Pol, 1999). Thus, the orexin system has been implicated in many brain functions and their involvement in the regulation of sleep, metabolic homeostasis and reward have been intensively studied (Tsujino and Sakurai, 2009).

While less well-studied, orexins are also antinociceptive. The antinociceptive action of orexin A given by *i.c.v.* or *i.v.*, but not *s.c.*, injection was first noted by Bingham et al. (2001). When given by *i.t.* injection, orexins also induced antinociception (Cheng et al., 2003; Mobarakeh et al., 2005). However, orexins are more potent antinoceptive agents when administered by *i.c.v.*, rather than *i.t.*, injection, in several pain models (Mobarakeh et al., 2005), suggesting a significant supraspinal contribution to orexin-induced antinociception (Chiou et al., 2010). The midbrain periaqueductal gray (PAG) is a likely supraspinal site of orexin antinociception. Orexin-containing fibers (Peyron et al., 1998), and OX1 and OX2 receptors are densely distributed in the PAG (Marcus et al., 2001), where *c-fos* expression was elevated when orexins were injected *i.c.v.* (Date et al., 1999).

Stimulating the ventrolateral PAG (vlPAG) results in antinociception (Behbehani et al., 1990) by activating a descending pain inhibitory pathway. Both opioid and cannabinoid systems contribute to the antinociception initiated from the vlPAG, which is enriched with opioid and cannabinoid receptors (Tsou et al., 1998; Yaksh et al., 1976). Endocannabinoids are particularly involved in the phenomenon of stress-induced analgesia (SIA) initiated in the PAG (Hohmann et al., 2005). Previously we have demonstrated that 2-arachidonoylglyceraol (2-AG), an endocannabinoid, can be generated after OX1 receptor activation in the rat vlPAG and contributes to the antinociceptive effect of intra-vlPAG injected orexin A (Ho et al., 2011). That is, orexin A activates postsynaptic OX1 receptors, via the GqPCR-coupled phospholipase C (PLC)-diacylglycerol lipase (DAGL) enzymatic pathway, to generate 2-AG that diffuses retrogradely back to activate presynaptic CB1 receptors on GABAergic terminals and inhibit GABA release in the vlPAG, leading to analgesia by increasing descending inhibition.

Endogenous orexins can play a role in the generation of SIA. During stress, hypothalamic orexin neurons are activated (Chang et al., 2007; Furlong et al., 2009; Mobarakeh et al., 2005; Rachalski et al., 2009; Sakamoto et al., 2004; Webb et al., 2008; Zhu et al., 2002). Watanabe et al. (Watanabe et al., 2005) found that footshocks reduced tail flick responses in normal mice but not in prepro-orexin knockout mice. Xie and colleagues (Xie et al., 2008) reported that restraint stress increased hot-plate nociceptive responses in normal mice but not in the mice with toxin-ablated orexin neurons.

We, therefore, examined the hypothesis that orexins released during stress might engage the OX1 receptor in the vlPAG, leading to endocannabinoid generation and the establishment of SIA. In rats, we (Ho et al., 2011) and Azhdari Zarmehri et al. (2011) have reported the antinociceptive effect of orexin A in the PAG in the hot-plate and formalin tests, respectively. In this study, we first reproduced the antinociceptive effect of orexins in the mouse vlPAG. Then, we clarified the relative contributions of OX1 and OX2 receptor subtypes and the involvement of endocannabinoids in the antinociceptive effect of orexins using pharmacological tools, including selective OX1 and OX2 antagonists, SB 334867 (Smart et al., 2001) and TCS-OX2-29 (Hirose et al., 2003), respectively, a selective OX2 agonsit, [Ala^{11}, D-Leu^{15}]-orexin B (AL-orexin B) (Asahi et al., 2003), and CB1 agonist and antagonist, WIN 55,212-2 (D'Ambra et al., 1992) and AM 251 (Gatley et al., 1996), respectively. Finally, we examined if this OX1 receptor-initiated and endocannabinoid-mediated antinociceptive mechanism contributes to SIA in restrained mice.

2. Materials and methods

All experiments adhered to the guidelines approved by the Institutional Animal Care and Use Committee of College of Medicine, National Taiwan University. Male C57BL/6 mice of 8–12 weeks were used. They were housed 5 per cage in a holding room with 12:12 light–dark cycle, 23 °C room temperature and food and water *ad libitum*. On the day of *in vivo* experiments, mice in their homecages were moved to a behavioral room and were acclimated there for 1 h before testing.

2.1. Hot-plate test

Paw withdrawal latencies to thermal stimulation on a hot plate of 50 °C were recorded. The withdrawal cut-off time was 60 s. To monitor the time course of an agonist-induced antinociception, the withdrawal latency was measured before (0 min) and 5, 10, 20, 30, 40, 50 and 60 min after intra-vlPAG drug administration. The antinociceptive effect was expressed as the percentage of maximal possible effect (%MPE): %MPE = 100 × (withdrawal latency$_{\text{after treatment}}$ - withdrawal latency$_{\text{before treatment}}$)/60 s - withdrawal latency$_{\text{before treatment}}$). The area under the curve (AUC) of the withdrawal latencies during the 60 min recording period was also calculated. The hot-plate test was always conducted in various treatment groups on the same day with the same number (2 or 3) of mice in each treatment group as well as a vehicle control group. The antinociceptive effect in each treatment group was normalized to the AUC of the vehicle group from the same day, and is summarized in the bar chart of the figures.

2.2. Intra-vlPAG microinjection

Mice were anesthetized with sodium pentobarbital (*i.p.* 80 mg/kg) and implanted with a 10 mm-long guide cannula 0.5 mm above the right vlPAG (AP: −4.8 mm, LM: −0.5 mm from midline, DV: −2.8 mm, from the skull surface) according to a mouse atlas (Paxinos and Watson, 1998). After cannulation, animals were returned to the holding room for at least 7 days to recover from the surgery.

On the day of behavioral testing, a 30-gauge injection cannula, connected to a 1 μl Hamilton syringe, was extended 0.5 mm beyond the tip of guide cannula for injecting the drug solution into the vlPAG. A microinfusion pump (KDS311, KD Scientific Inc.) was used to deliver the drug solution of 0.1 μl over 1 min. The injection cannula was left at the injection site for an additional 4 min to allow for complete diffusion of the injected drug. When a receptor antagonist was co-injected with orexin A or AL-orexin B, two fold-concentrated drug solutions were prepared to keep the injection volume at 0.1 μl. Specifically, antagonist solution, 0.05 μl, was injected followed by 0.05 μl of orexin A or AL-orexin B solution. The selection of injected doses was based on our previous study (Ho et al., 2011) with modification. To confirm the microinjection site, a 0.4% trypan blue solution was injected through the cannula after behavioral tests (Supplementary Fig. 1). If the injection site confirmed in fixed midbrain slices (50 μm) was outside the vlPAG (offsite injection), no antinociceptive effect was observed and the data from that mouse was excluded in behavioral analysis. The percentage of offsite injection was less than 7%.

2.3. Restraint stress model

Mice were randomly separated into restrained and control groups. The restrained mouse was put into a centrifuge tube (50 c.c.) with several small holes, which kept the mouse from overheating, for 30 min. Antagonsits were given by either

intraperitoneal (*i.p.*) injection 15 min or intra-vlPAG microinjection (*i.pag.*) 5 min before restraint stress. The hot-plate latency in the mouse was measured in this set of experiments before antagonist treatment, before restraint and 0, 15 and 30 min after restraint stress. Immunohistorical staining of c-FOS protein in the lateral hypothalamus (LH) of the mouse was performed 2 h after restraint stress. Orexin A levels in the vlPAG as well as plasma corticosterone levels were measured immediately after restraint stress. Unrestrained control mice were held in their home cages in the behavioral room for an equivalent 30 min.

2.4. Immunohistochemistry in the LH

Two hours after restraint stress, mice were anesthetized with sodium pentobarbital (*i.p.* 80 mg/kg) and then sacrificed by intracardiac perfusion with 4% paraformaldehyde. After perfusion, the whole brain was dissected, post-fixed for 2 days in the same fixative and cryoprotected in 30% sucrose for at least 2 days. Brains were embedded in OCT and cut on a cryostat (Leica CM3050 S) for acquiring coronal sections (50 μm) of the entire hypothalamus. Double-label immunohistochemistry of c-Fos and orexin A was carried out in every fourth serial section (50 μm) along the coronal axis of the hypothalamus. The sections were treated with 1% NaBH4 in 0.1 M phosphate buffer (PB) for 20 min, and then with 0.5% H_2O_2 in PB for 30 min. Sections were blocked with 5% normal goat serum (NGS) and 0.2% TritonX-100 at room temperature for 1 h and then incubated in a cocktail of sheep anti-c-Fos (1:2000; ab6167, Abcam, Cambridge, MA) and rabbit anti-orexin A (1:1000; H-003-30, Phoenix Pharmaceuticals, Burlingame, CA) antibodies for 48 h. Following three washes in PB, sections were reacted with biotinylated anti-rabbit IgG antibody (1:200; Vector laboratories, Burlingame, CA) for 2 h, and then with alkaline phosphatase conjugated anti-sheep IgG (1: 200; ab6748, Abcam) for 2 h at room temperature. Orexin A immunostaining was developed with the use of the avidin–biotin–peroxidase complex (1:200) and a 3, 3'-diaminobenzidine substrate kit (Vector Laboratories). The same sections were then processed for c-Fos immunostaining with VectorR Blue kit (Vector Laboratories). Sections were mounted with glycerol onto gelatin-coated slides. Immunohistochemical control experiments were performed with omission of the primary antiserum and staining was absent in all control experiments.

2.5. Stereological analysis

Consecutive sections, 200 μm apart, covering the entire LH were analyzed on one side, left or right. All orexin A single-labeled and c-Fos and orexin A double labeled neurons were counted by the StereoInvestigator (MicroBrightField, CA) with a 60 × objective.

2.6. Enzyme immunoassay (EIA) of orexin A in the vlPAG homogenate

Immediately after restraint stress, the mouse was sacrificed and its brain was immediately removed and placed on its dorsal surface in a pre-cooled stainless steel adult mouse brain slicer matrix (Roboz Surgical Instrument, Gaithersburg, MD), and sliced into 1 mm-thick coronal sections. The slicer matrix was kept in an ice bath throughout the slicing procedure. The vlPAG brain tissues were bilaterally punched out with a 0.5 mm-tip Harris Micro-Punch tool (Ted Pella Inc, Redding, CA), according to a mouse brain atlas (Franklin and Paxinos, 1997). Brain tissue samples were then homogenized in ice-cold lysis buffer, by an ultrasonicator (VCX 750; Sonics &. Materials, Inc., Newtown, CT) for 2 min. The lysis buffer contained 50 mM Tris–HCl pH 7.4, 150 mM NaCl, 1% nonyl phenoxypolyethoxylethanol, 1 mM EDTA, 0.25% sodium deoxycholate and phosphatase (PhosSTOP, Roche, Germany) and protease (Complete mini, Roche, Germany) inhibitor cocktails. The lysates were then homogenized and centrifuged (14000 rpm, 15 min) and supernatants were collected. The protein concentration in the supernatant was measured by the Bradford method (Bradford, 1976). Orexin A levels in these vlPAG homogenates were measured using a commercially available chemiluminescent EIA kit (Cat. No. CEK-003-30, Lot No. 604124, Phoenix Pharmaceuticals, Inc., Burlingame, CA).

2.7. Measurement of plasma corticosterone levels

Immediately after restraint stress, the mouse was decapitated and its trunk blood was collected in a tube containing 3.8% sodium citrate. Plasma samples were prepared by centrifugation at 1000× *g* for 15 min. Plasma corticosterone levels were measured by a commercial EIA kit (Cat. No. 500655, Lot No. 0418058, Cayman Chemical Co., Ann Arbor, MI).

2.8. Chemicals

Orexin A, AL-orexin B, SB 334867 and TCS-OX2-29 were purchased from Tocris Bioscience (Bristol, UK). Naloxone, naltrexone, WIN 55,212-2 and AM 251 were bought from Sigma–Aldrich (St. Louis, MO). Morphine sulfate was purchased from Division of Controlled Drugs, Food and Drug Administration, Department of Health, Executive Yuan, Taiwan. Orexin A, AL-orexin B, morphine, TCS-OX2-29, naloxone and naltrexone were dissolved in normal saline. For *i.pag.* microinjection, SB 334867, WIN 55,212-2 and AM 251 were dissolved in dimethylsulfoxide (DMSO). For *i.p.* injections, SB334867 and AM 251 were dissolved in a water solution containing 10% (w/v) encapsin and 2% (v/v) DMSO. All drugs were prepared at the working concentrations for either *i.pag.* microinjections or *i.p.* injections. The *i.p.* injection volume was 10 ml/kg.

2.9. Statistics

Data are expressed as the mean ± S.E.M and the *n* number indicates the number of the mice tested in each group. In the hot-plate test, non-parametric statistical analyses were used. Comparisons between two groups were analyzed by Mann–Whitney test and among three groups or more by Kruskal–Wallis test with the *post hoc* Tukey test. Non-parametric repeat measures two-way ANOVA with *post hoc* Bonferroni test was used for the analysis of time courses of antinociceptive effects among different groups. One sample *t*-test was used to analyze the percent increment in the AUC. In experiments measuring activated orexin neuronal numbers, orexin A levels and corticosterone levels, Student's *t-test* was used. Differences were considered significant if $p < 0.05$.

3. Results

3.1. Intra-vlPAG microinjection of orexin A reduced hot-plate nociceptive responses in mice

When given by *i.pag.* microinjection, orexin A, at 0.01–1 nmol, increased the withdrawal latency in the mouse hot-plate test in a time- ($F_{7,128} = 10.36$, $p < 0.001$, two-way ANOVA, Fig. 1A) and dose-dependent ($F_{4,128} = 59.29$, $p < 0.001$, two-way ANOVA, Fig. 1A) manner. When the *i.pag.* dose of orexin A was increased to 3 nmol, the spontaneous locomotor activity of mice was slightly decreased. Thus, the maximal achievable antinociceptive effect without motor impairment was produced by 1 nmol orexin A, reaching 75% MPE at 5 min after injection, and then decreasing by 20 min to around 40% MPE, and persisted at that level for 60 min (Fig. 1A, filled circles).

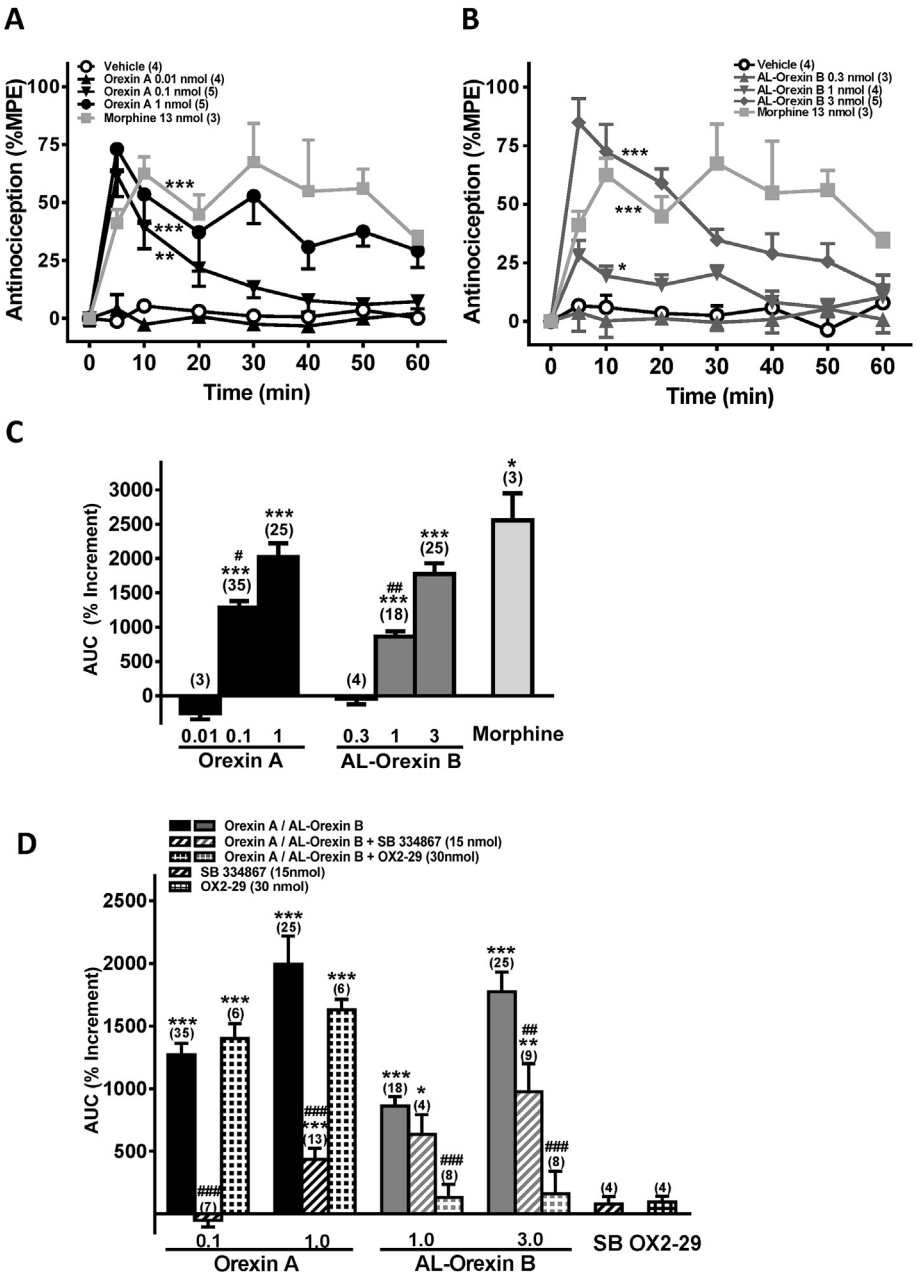

Fig. 1. Antinociceptive effects of intra-vlPAG (i.pag.) microinjection of orexin A, [Ala[11], D-Leu[15]]-orexin B (AL-orexin B) and morphine and their interactions with OX1, OX2 and opioid receptor antagonists in the mouse hot-plate test. (A–B) Time courses of antinociceptive effects of 0.01–1 nmol orexin A (A), 0.3–3 nmol AL-orexin B (B), and 13 nmol morphine. The antinociceptive effect is expressed as percentage of the maximal possible effect (MPE): %MPE = 100% × (withdrawal latency$_{\text{after treatment}}$ − withdrawal latency$_{\text{before treatment}}$)/60 s − withdrawal latency$_{\text{before treatment}}$). Data are the average antinociceptive effect in each treatment group at the same time point. $^{**}p < 0.01$, $^{***}p < 0.001$ vs. the vehicle group (Repeat measures two-way ANOVA with post hoc Bonferroni test). (C) Antinociceptive effects of 0.01–1 nmol orexin A, 0.3–3 nmol AL-orexin B and 13 nmol morphine. (D) Antinociceptive effects of 15 nmol SB 334867 (SB, an OX1 antagonist) and 30 nmol TCX-OX2-29 (OX2-29, an OX2 antagonist) alone or in combination with 0.1–1 nmol orexin A or 1–3 nmol AL-orexin B. In each group of bars, mice with the same number (2 or 3) in each treatment group as well as a vehicle group received the hot-plate test on the same day. The ordinate is the antinociceptive effect expressed as the percent increment of the area under the curve (AUC) of the withdrawal latencies during the 60 min-recording period in each treatment group after normalized to the AUC of the respective vehicle-treated group. The numbers in the parentheses include all mice in each group that were tested. $^{*}p < 0.05$, $^{**}p < 0.01$, $^{***}p < 0.001$ vs. the vehicle group, i.e. zero increment in AUC (one sample t-test); $^{\#}p < 0.05$, $^{\#\#}p < 0.01$, $^{\#\#\#}p < 0.001$ vs. the group treated with orexin A or AL-orexin B only (Mann–Whitney test). The same data presentation and statistical analysis apply to Figs. 2–3.

The maximal effect induced by 1 nmol orexin A was comparable to that produced by morphine in the vlPAG, at the dose (13 nmol) that has been reported to be an effective antinociceptive dose in the PAG of C57 mice (Nunes-de-Souza et al., 1991), while the effect of morphine lasted longer (Fig. 1A, C).

3.2. AL-orexin B was also antinociceptive but was 3-fold less potent than orexin A

Effects of AL-orexin B at 0.3, 1, 3 and 10 nmol on the mouse hot-plate latency were examined. AL-orexin B displayed a significant antinociceptive effect at 1 and 3 nmol (Fig. 1B, C). As described above, *i.pag.* orexin A at higher doses impaired motor activity, it is

not feasible to compare the antinoicicpetive ED50s between orexin A and AL-orexin B. However, comparing their doses producing comparative antinociceptive effects, it seems that AL-orexin B is less potent than orexin A. The AUC increment (1774 ± 155% of control) induced by 3 nmol AL-orexin B was comparable to that (2018 ± 202% of control) produced by 1 nmol orexin A (Fig. 1C) ($p = 0.3441$, Mann–Whitney test). Thus, AL-orexin B was about 3-fold less potent than orexin A. AL-orexin B (3 nmol) also produced antinociceptive effect immediately (5 min) after injection, however, its effect decayed faster than that produced by orexin A (1 nmol) (Fig. 1B *vs.* Fig. 1A).

3.3. The effect of orexin A was mediated through OX1, but not OX2, receptors

SB 334867 (*i.pag.*, 15 nmol) when co-injected with orexin A into the vlPAG, completely abolished the effect of 0.1 nmol orexin A, but with 1 nmol orexin A a residual analgesic effect remained (2nd paired columns, Fig. 1D). On the other hand, TCS-OX2-29 (*i.pag.*, 30 nmol), an OX2 receptor selective antagonist (Hirose et al., 2003), did not affect the effect of orexin A at 0.1 nmol and slightly, though insignificantly, reduced its effect at 1 nmol (Fig. 1D). Neither SB 334867 nor TCS-OX2-29 *per se* changed the hot-plate latency (Fig. 1D).

3.4. The effect of AL-orexin B was mediated by OX2 receptors and, at higher doses, also by OX1 receptors

SB-334867 (15 nmol) did not affect the antinociceptive effect of 1 nmol AL-orexin B, but significantly reduced the effect of 3 nmol AL-orexin B (Fig. 1D). TCS-OX2-29 (30 nmol) effectively antagonized effects of AL-orexin B at both 1 and 3 nmol (Fig. 1D).

3.5. The opioid system was not involved in the antinociceptive effects of orexin A and AL-orexin B

Opioid receptors and endorphins are enriched in the vlPAG (Guo et al., 2004). To elucidate if orexins induce antinociception indirectly by activating the opioid system, the effect of naloxone on orexin antinociception was examined. Neither the antinociceptive effect of orexin A nor that of AL-orexin B was affected by naloxone at the dose (5 nmol) that effectively antagonized morphine-induced antinociception (Fig. 2). Naloxone *per se* did not change the hot-plate latency (Fig. 2).

3.6. The antinociceptive effect of orexin A, but not AL-orexin B, was inhibited by a CB1 antagonist and mimicked by a CB1 agonist

In previous study, we found that, an endocannabinoid (2-AG) can be generated after OX1 receptor activation via Gq-protein-coupled phospholipase C (PLC) and subsequent diacylglyceral lipase (DAGL) activation, and this endocannabinoid-mediated inhibition of GABAergic transmission in the vlPAG contributes to the antinociceptive effect of intra-vlPAG orexin A in rats (Ho et al., 2011). Here, we examined whether endocannabinoids also play a role in the antinociceptive effects of intra-vlPAG injected orexin A and AL-orexin B in mice. Intra-vlPAG microinjection of WIN 55,212-2 (30–100 nmol), a CB1 receptor agonist, reduced the hot-plate nociceptive response in mice (Fig. 3). The efficacy of WIN 55,212-2 at 100 nmol, however, was less than that of orexin A (1 nmol) or AL-orexin B (3 nmol) (Fig. 3). AM 251, a CB1 antagonist, at a dose (30 nmol) that effectively antagonized WIN 55,212-2-induced antinociception, completely abolished the antinociceptive effect of 0.1 nmol orexin A and significantly reduced the effect of 1 nmol orexin A (Fig. 3). The effect of AL-orexin B at 3 nmol was not significantly affected by AM 251 (Fig. 3). AM 251 *per se* had no effect on the hot-plate latency (Fig. 3).

3.7. Restraint stress induced SIA in a manner blocked by CB1 and OX1 antagonists

Xie et al. (2008) have reported that a 30 min-restraint stress SIA was diminished in mice with toxin-ablated orexin neurons, suggesting this SIA is orexin-dependent. First, we validated this restraint SIA model in our mice. Indeed, mice receiving a 30 min-restraint stress showed significantly longer withdrawal latency in the hot-plate test, as compared with the unrestrained group (21.12 ± 2.9 *vs.* 2.8 ± 1.4%MPE, $p < 0.01$) (Fig. 4). The antinociceptive effect induced by restraint stress was significantly prevented by *i.p.* injection of 15 mg/kg SB 334867 (Fig. 4A) or 1.1 mg/kg AM 251 (Fig. 4B), while neither SB 334867 nor AM 251 affected hot-plate latencies in unrestrained control mice. This restraint SIA was

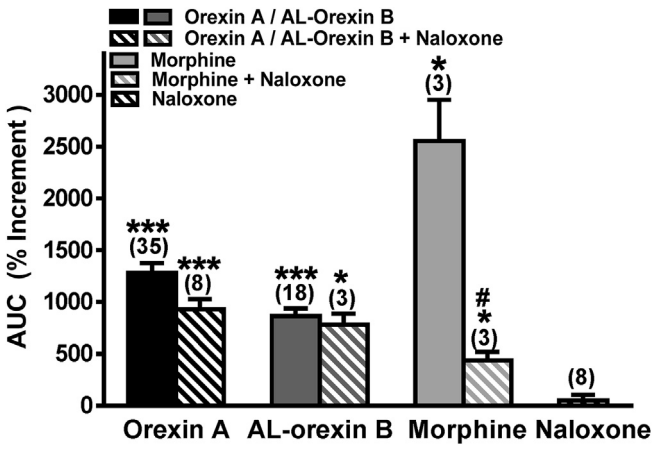

Fig. 2. Antinociceptive effects of orexin A and AL-orexin B in the vlPAG were opioid-independent. Antinociceptive effects of 5 nmol naloxone (an opioid receptor antagonist) alone or in combination with 0.1 nmol orexin A, 1 nmol AL-orexin B, or 13 nmol morphine. The data presentation and statistics are the same as in Fig. 1D. $^{*}p < 0.05$, $^{***}p < 0.001$ vs. the vehicle group, $^{\#}p < 0.05$ vs. the group treated with the agonist only.

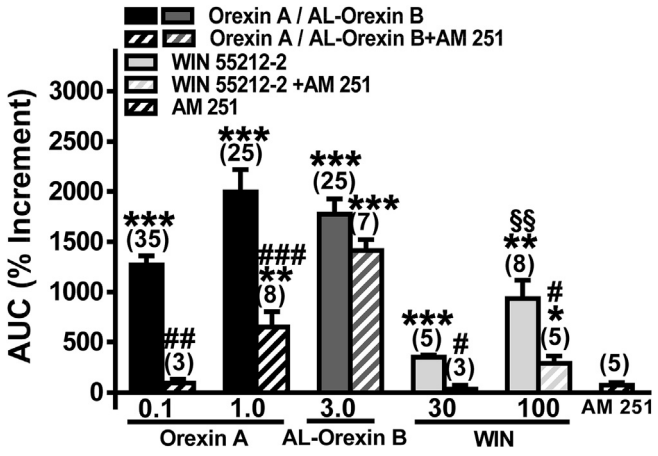

Fig. 3. The antinociceptive effect of orexin A, but not AL-orexin B, was mediated by endocannabinoid-CB1 receptor signaling in the vlPAG. Antinociceptive effects of 30 nmol AM 251 (a CB1 antagonist) alone or in combination with 0.1–1 nmol orexin A, 3 nmol AL-orexin B, or 30–100 nmol WIN 55,212-2, a CB1 agonist. The data presentation and statistics are the same as in Fig. 1D. $^{*}p < 0.05$, $^{***}p < 0.001$ vs. the vehicle group; $^{\#}p < 0.05$, $^{\#\#}p < 0.01$, $^{\#\#\#}p < 0.001$ vs. the group treated with the agonist only, $^{\S\S}p < 0.01$ vs. the group treated with 1 nmol orexin A only.

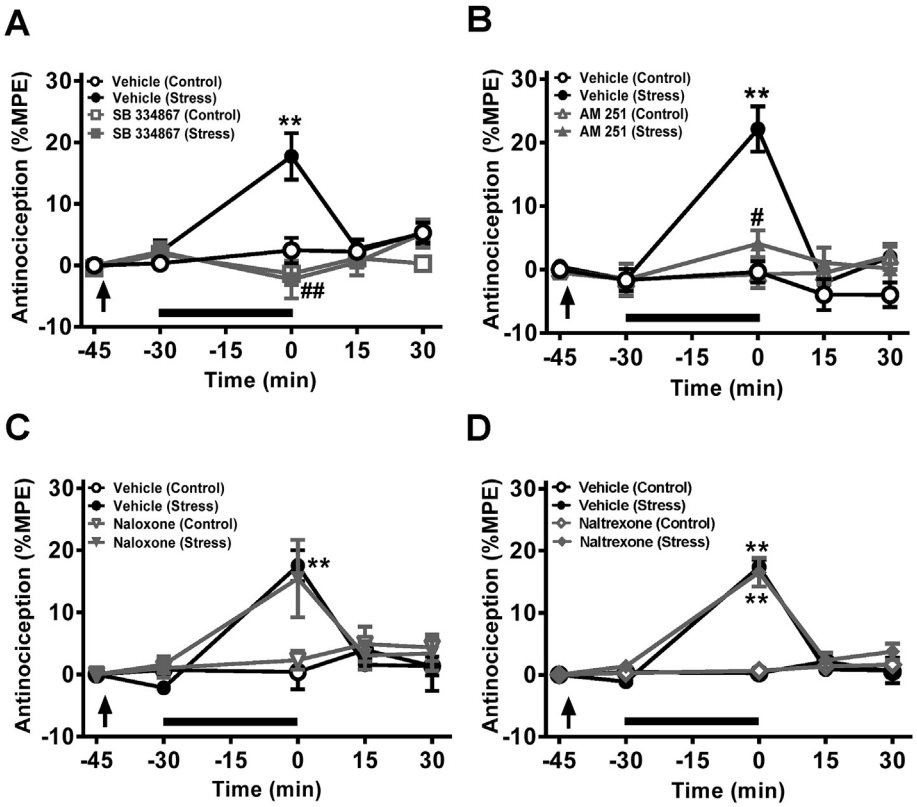

Fig. 4. OX1 and CB1, but not opioid, receptor antagonists inhibited restraint stress-induced analgesia (SIA) in mice. Restraint stress was induced by placing the mouse into a 50 ml perforated centrifuge tube for 30 min. The control group remained in their home cages. Effects of ip. injection of 15 mg/kg SB 334867 (an OX1 antagonist) (A), 1.1 mg/kg AM 251 (a CB1R antagonist) (B), 1 mg/kg naloxone (C) (an opioid receptor antagonist) and 1 mg/kg naltrexone (a long-acting opioid receptor antagonist) (D), and their respective vehicles on the hot-plate test in restrained and control mice. The ordinate is the antinociceptive effect in various groups, expressed as %MPE as described in Fig. 1A, B. Note that a significant antinociceptive effect was induced in restrained mice, an SIA phenomenon, which was blocked by SB 334867 or AM 251, but not by naloxone or naltrexone. All drugs or vehicles were given by i.p. injection 15 min (arrows) before restraint stress (thick bars). $^{**}p < 0.01$ vs. the control unrestrained group, $^{\#}p < 0.05$, $^{\#\#}p < 0.01$ vs. the vehicle group, at time 0 (Two way ANOVA with post hoc Tukey test) (n = 6).

unaffected by *i.p.* injection of 1 mg/kg naloxone (Fig. 4C). Since naloxone is quickly metabolized (Berkowitz, 1976), we further examined the effect of a long-acting opioid receptor antagonist, naltrexone. Similarly, *i.p.* injection of 1 mg/kg naltrexone also had no effect on SIA (Fig. 4D).

The restraint SIA was also abolished by *i.pag.* microinjection of SB 334867 (15 nmol, Fig. 5A) or AM 251 (30 nmol, Fig. 5B), but not TCS-OX2-29 (30 nmol, Fig. 5C). These receptor antagonists had no effect *per se* in unrestrained control mice. These results suggest that during restraint stress, OX1, but not OX2, receptors in the vlPAG are activated by endogenous orexins to reduce the hot-plate nociceptive response in restrained mice via CB1 receptors. Interestingly, the antinociceptive effect induced by restraint stress (21.1% ± 2.9% MPE, Fig. 5) was much smaller than that (61.7% ± 9.1% MPE, Fig. 1A) produced by direct microinjection of orexin A (0.1 nmol) into the vlPAG.

3.8. Restraint stress increased c-Fos positive LH orexin neurons

The *c-fos* gene, an immediate early gene, is believed to be transcribed when neurons are strongly activated (Sagar et al., 1988). Expression of c-Fos protein in activated neurons can be measured 2 h after neuronal activation. According to a previous study (Johnson et al., 2010), activated orexin neurons can be revealed by the presence of double-immunoreactivity of c-Fos and orexin in the same neuron, i.e. c-Fos immunoreactivity in the nucleus and orexin immunoreactivity in the cytosol. Fig. 6 shows that the number of c-Fos-expressing orexin neurons, revealed by the double-immunolabeled neurons (arrows in Fig. 6A, B), in LH sections were markedly increased in the restrained group, as compared to the unrestrained control group. Most orexin neurons in the control group were free of c-Fos staining (arrow heads in Fig. 6A). The percentage of orexin neurons double-immunolabeled with c-Fos was significantly higher in the restrained group than in the control group (Fig. 6C), while the total number of orexin neurons was not different between two groups (Fig. 6D).

3.9. Restraint stress elevated the orexin A level in the vlPAG and the plasma corticosterone level

The average orexin A level in vlPAG homogenates isolated from restrained mice was significantly higher than that from unrestrained mice (Fig. 7A). Additionally, the plasma levels of corticosterone, a stress hormone, in restrained mice were significantly elevated, as compared with control mice (Fig. 7B). Interestingly, SB 334867 (*i.p.*, 15 mg/kg), although abolishing restraint SIA, did not affect the restraint stress-induced elevation in corticosterone levels (Fig. 7B).

4. Discussion

In this study, we demonstrated that activation of the OX1 receptor in the vlPAG of mice can initiate an endocannabinoid-CB1 receptor-mediated analgesia, as we observed in rats (Ho et al.,

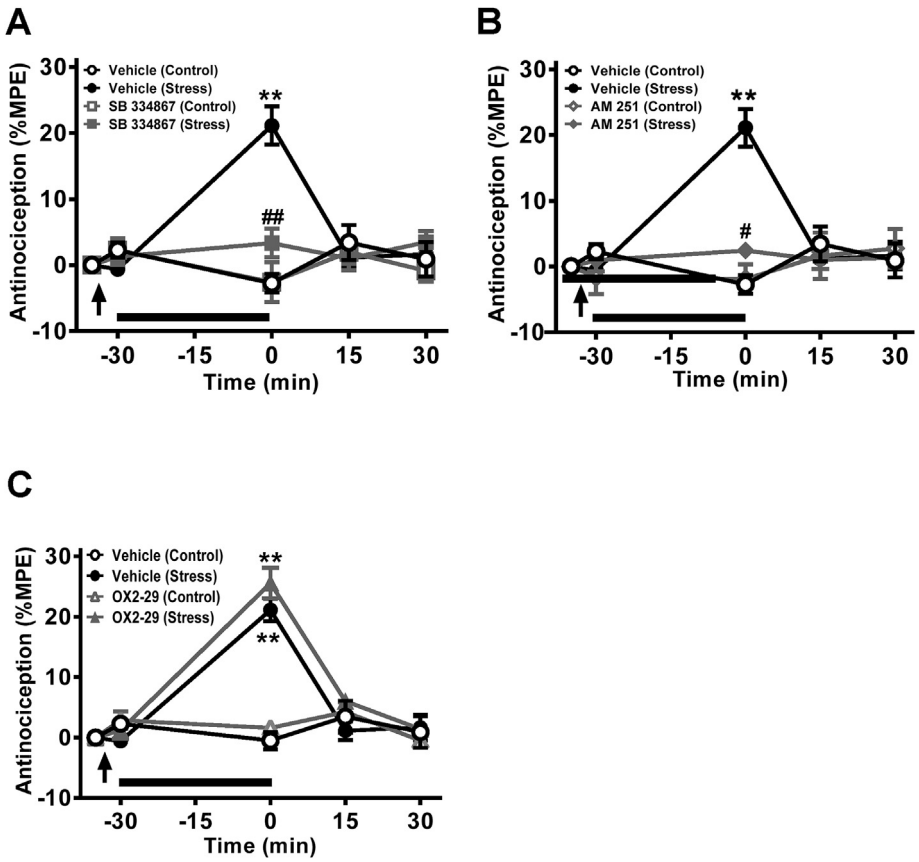

Fig. 5. The OX1 and CB1, but not OX2 receptor, antagonist given by i.pag. microinjection inhibited restraint SIA in mice. Effects of i.pag. microinjection of 15 nomol SB 33486 (A), 30 nmol TCS-OX2-29 (OX2-29) (B) and 30 nmol AM 251 (C), and their respective vehicles on the hot-plate test in restrained and control mice. The ordinate is the antinociceptive effect in various groups, expressed as %MPE as described in Fig. 1A, B. All drugs and vehicles were given by i.pag. microinjection 5 min (arrows) before restraint stress (thick bars). $^{**}p < 0.01$ vs. the control unrestrained group, $^{\#}p < 0.05$, $^{\#\#}p < 0.01$ vs. the vehicle group, at time 0 (Two way ANOVA with post hoc Tukey test) ($n = 6$).

2011). Activation of the OX2 receptor in the vlPAG is also antinociceptive but this antinociceptive effect is CB1 receptor-independent. The OX1 receptor-initiated, endocannabinoid-mediated disinhibition mechanism in the vlPAG revealed in our previous study (Ho et al., 2011) may contribute to the antinociceptive effect induced not only by *i.pag.* injected orexin A in mice but also, more importantly, by endogenous orexins released from the LH during restraint stress. To the best of our knowledge, this is the first study revealing the contribution of a sequential activation of orexin and endocannabinoid systems in SIA.

4.1. The vlPAG is the site of supraspinal antinociceptive action of orexins

Orexin A and orexin B given by *i.c.v.* injection have been reported to be antinociceptive in several animal models of pain (Chiou et al., 2010). The current study suggests the vlPAG is an important supraspinal action site for orexin-induced antinociception in mice, in agreement with our previous finding in rats (Ho et al., 2011). Azhdari Zarmehri et al. (2011) also demonstrated that intra-PAG microinjection of orexin A produced an OX1-receptor mediated antinociception in the rat formalin test.

In addition to the PAG (Azhdari Zarmehri et al., 2011; Chiou et al., 2010; Ho et al., 2011), orexin A was recently reported to reduce the nociceptive response in the formalin-inflammed rat when given at several brain regions, including the rostral ventromedial medulla (Azhdari-Zarmehri et al., 2014), paragigantocellularis lateralis (Erami et al., 2012) and locus ceoleus (Mohammad-Pour Kargar et al., 2015). The ventral tegmental acrea and nucleus accumbens were also reported to be involved in the antinociception induced by stimulating the lateral hypothalamus (Azhdari-Zarmehri et al., 2013; Sadeghi et al., 2013). Orexins are potent neuronal stimulators and could inevitably activate those brain regions when given by local injection. It remains to be elucidated whether endogenous orexins under certain physiological or pathological conditions can be released to produce antinociception in these brain regions.

4.2. The antinociceptive effect of orexin A is mediated through OX1, but not OX2 or opioid receptors

Orexin A-induced antinociception in the mouse vlPAG is mainly mediated by OX1, but not OX2, receptors since it was significantly prevented by *i.pag.* SB 334867, but not TCS-OX2-29. A significant residual effect of orexin A at a higher dose, 1 nmol, in the presence of 15 nmol SB 334867 (2nd grouped-columns in Fig. 1D) might be resulted from its effect on the receptor other than OX1 since the dose ratio of SB 334867 to orexin A (15:1) is much higher than their Kd ratio (3: 1) at OX1 receptors (Smart et al., 2001). The contribution of OX2 receptor in this effect of orexin A cannot be ruled out since TCS-OX2-29 also tended to reduce it (2nd grouped-columns in Fig. 1D). The ineffectiveness of both OX1 and OX2 antagonists alone suggests that endogenous orexins might not be operative in the vlPAG in this hot-plate acute pain model. However, endogenous orexins do play a role in SIA (see below).

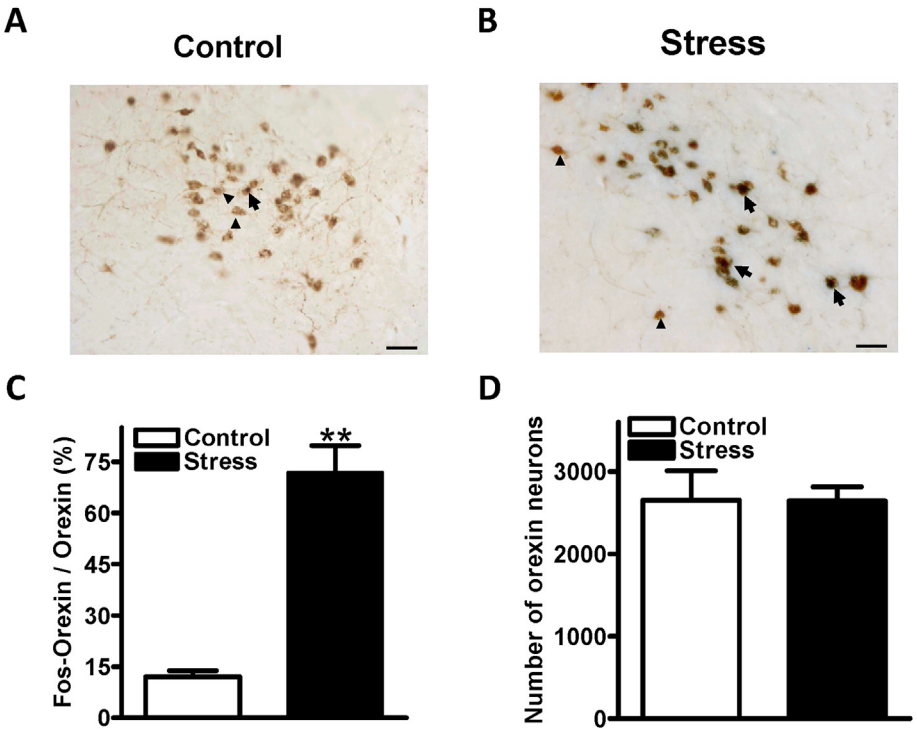

Fig. 6. Restraint stress increased the number of c-Fos-expressing orexin neurons in the lateral hypothalamus (LH). Double immunolabeling of c-Fos protein and orexin A in LH neurons was conducted in tissues harvested 2 h after termination of restraint stress from mice subjected to a 30 min-restraint stress (Stress) or from unrestrained control mice (Control). (A–B) A representitive LH section taken from control (A) or restrained (B) mice. Orexin A was labeled by DAB in brown color and c-Fos was labeled by VectorR Blue in blue gray color. Note that there were more double immunolabeled neurons (arrows) in the stress group as compared to the control group, in which most orexin A-immunoreactive neurons were free of c-Fos staining (arrowheads). Calibration bar: 50 μm. (C–D) The percentage of orexin A neurons expressing c-Fos (C) and the total number of orexin A-immunoreactive neurons (D) in both groups (n = 3). The number of orexin A- and c-Fos-immunoreactive neurons was calculated using StereoInvestigator from a series of 50 μm-think sections taken every 200 μm along the coronal axis of a mouse hemi-hypothalamus. **p < 0.01 vs. the Control group (Student's t test). (For interpretation of the references to colour in this figure legend, the reader is referred to the web version of this article.)

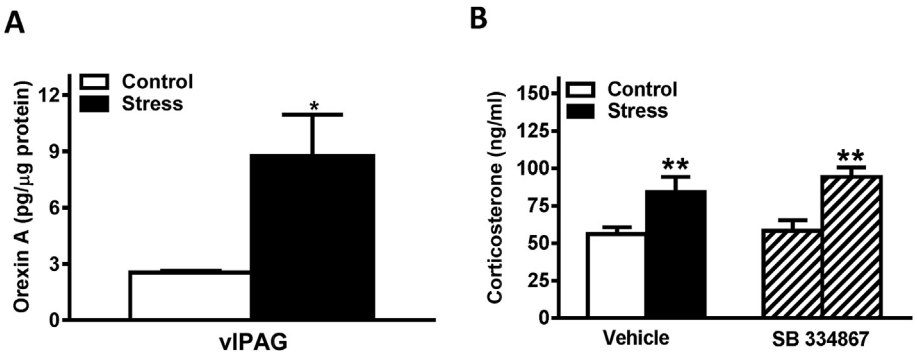

Fig. 7. Restraint stress increased the orexin A level in the vlPAG homogenate and the plasma corticosterone level. (A) Orexin A levels in vlPAG homogenates of restrained and control unrestrained mice. Brain tissues containing the vlPAG were punched and homogenized from restrained mice immediately after a 30 min-restraint stress or from unrestrained control mice. Orexin A levels in vlPAG homogenates were measured by an EIA kit (Phoenix Pharmaceuticals, Inc.), n = 4. (B) Corticosterone levels of restrained and control mice treated with SB 334867 or its vehicle. Corticosterone levels in plasma samples that were collected in restrained mice immediately after restraint stress or from unrestrained control mice and measured by an EIA kit (Cayman Chemical Co.), n = 5. SB 334867 (15 mg/kg) was given by i.p. injection 15 min before implementing restraint stress. *p < 0.05, **p < 0.01 vs. the Control group (Student's t test).

4.3. The antinociceptive effect of AL-orexin B is mainly mediated through OX2 receptors unless at higher doses

AL-Orexin B was reported to be 400 times more selective at OX2 receptors than at OX1 receptors (Asahi et al., 2003). The finding that TCS-OX2-29 significantly antagonized the antinociceptive effect of AL-orexin B suggests that activating the OX2 receptor in the vlPAG is also nociceptive and the effect of AL-orexin B is mainly mediated by OX2 receptors. However, at a higher dose (3 nmol), the effect of AL-orexin B was partially reduced by SB 334867, suggesting that the OX1 receptor also contributes to the antinociceptive effect induced by a high dose of AL-orexin B.

4.4. Antinociceptive effects of orexins are opioid-independent

Although endogenous opioids are enriched in the vlPAG and play an important role in the antinociception initiated in this region, the antinociceptive effect of neither orexin A nor AL-orexin B

was antagonized by naloxone at a dose that effectively antagonized the effect of morphine (Fig. 2). This suggests that the anti-nociceptive effect of orexins in the vlPAG is opioid-independent.

4.5. Activation of OX1, but not OX2, receptors in the vlPG initiates an endocannabinoid-CB1 receptor-mediated analgesia

We have previously demonstrated that activation of the OX1 receptor in rat PAG slices initiates the synthesis of 2-AG, an endocannabinoid, via a Gq-PLC-DAGL signaling cascade to inhibit GABAergic transmission. This endocannabinoid-mediated disinhibition mechanism in the vlPAG contributes to the antinociceptive effect of intra-vlPAG orexin A in rats (Ho et al., 2011). Endocannabinoids can be synthesized on demand and reduce nociceptive responses (Maione et al., 2006; Walker et al., 1999). In this study, the finding that the antinociceptive effect of orexin A was markedly reduced by a CB1 antagonist and mimicked by a CB1 agonist suggests that this OX1 receptor-initiated endocannabinoid-mediated mechanism also plays a role in orexin A-induced antinociception in mice. The possibility that AM 251 directly block OX1 receptors can be excluded by our previously finding that AM 251 did not affect OX1 receptor-mediated membrane depolarization induced by orexin A (Ho et al., 2011).

Interestingly, the antinociceptive effect of AL-orexin B was not significantly affected by AM 251, suggesting the OX2 receptor-mediated antinociception in the vlPAG is independent of the endocannabinoid-CB1 receptor system. With a higher dose of orexin A (1 nmol), a significant residual antinociceptive effect was observed in the presence of AM 251 (2nd paired-columns in Fig. 3). This could be an effect independent of OX1 receptors, as the result observed in Fig. 1D (2nd grouped-columns), and could possibly be mediated by OX2 receptors. It could also be an OX1 receptor-mediated, but endocannabinoid-independent effect of orexin A, such as postsynaptic OX1 receptor-mediated depolarization (Ho et al., 2011).

4.6. Restraint stress activates LH orexin neurons and produces analgesia through the OX1 receptor-initiated endocannabinoid-CB1 signaling in the vlPAG

The findings that *i.pag.* microinjection of either SB 334867 or AM 251 prevented restraint SIA suggest that, during restraint stress, endogenous orexins are released and produce analgesia through the OX1 receptor-initiated endocannabinoid-CB1 signaling in the vlPAG. Orexins are very likely released from neurons originating in the LH since restraint stress increased the number of activated LH orexin neurons (Fig. 6). This restraint SIA in mice is opioid-independent since neither naloxone nor naltrexone affected it while it is mediated through OX1 and CB1 receptors, and possibly involves 2-AG in the vlPAG (Ho et al., 2011). Interestingly, Hohmann et al. (2005) reported that a 3-min continuous foot shock in rats induced an SIA mediated by both anandamide and 2-AG via CB1 receptors in the dorsolateral PAG. The reason for this discrepancy is unclear, but is not due to species difference. We found orexin A was ineffective if intentionally injected in the dorsolateral PAG of rats (Ho et al., 2011). It seems that OX1 receptor-mediated analgesia within the vlPAG involves only 2-AG. The stress condition in our study (restraint) is also different from that (foot shock) used in the study of Hohmann et al. (2005). Stress-induced orexins could induce analgesia via 2-AG synthesis either directly in vlPAG projection neurons (Ho et al., 2011) or indirectly by increasing mGluR5-mediated glutamatergic transmission (Gregg et al., 2012), after OX1 receptor activation.

It has been reported that orexin neurons in the LH can be activated by restraint stress in hamsters (Webb et al., 2008), mice (Rachalski et al., 2009) and rats (Sakamoto et al., 2004) as well as by other stress conditions (Chang et al., 2007; Mobarakeh et al., 2005; Sakamoto et al., 2004; Zhu et al., 2002). We also found that restraint stress markedly increased the number of activated LH orexin neurons (Fig. 6) and orexin A levels in the vlPAG (Fig. 7A). Interestingly, the maximal antinociceptive effect induced by restraint stress, in terms of %MPE, was much less than that produced by intra-vlPAG injected 0.1 nmol orexin A (Figs. 4 and 5 *vs.* Fig. 1A). This suggests that a limited amount of orexins were released during restraint stress; however this amount is sufficient to elicit SIA. Restraint stress also activates the hypothalamic-pituitary-adrenal (HPA) axis, reflected by elevated corticosterone levels in restrained mice, in a manner unaffected by SB 334867 (Fig. 7B). This suggests that restraint stress activates the HPA axis is not downstream of OX1 receptor activation. Recently, Gerashchenko et al. (2011) found that nociceptin inhibited hypothalamic orexin neurons in the perifonical area, leading to inhibition of restraint SIA in rats. This can explain the pronociceptive effect induced by nociceptin if given by *i.c.v.* injection, when animals were under stress (Grisel et al., 1996). It remains to be elucidated if the pronociceptive effect of nociceptin can be blocked by enhancing 2-AG signaling via inhibiting its degradation enzyme, monoacylglycerol lipase.

In summary, our results suggest that during stress, hypothalamic orexin neurons are activated, releasing orexins to activate the OX1 receptor in the vlPAG and induce analgesia likely via a disinhibition mechanism in the vlPAG mediated by 2-AG.

Acknowledgments

This study was supported by the grants from the National Health Reserach Institutes, Taiwan (NHRI-EX104-10251NI) and the Ministry of Science and Technology, Taiwan (MOST103-2321-B002-035, MOST104-2745-B002-004, MOST104-2325-B002-010, MOST104-2314-B002-053-MY3 and MOST 104-2923-B002-006-MY3) to L.-C.C., and grants from the US National Institutes of Health to K.M. (DA021696 and DA011322). We thank the support from Dr. Li-Jen Lee, Dept. Anatomy and Cellular Biology, National Taiwan University and the Core Labs in College of Medicine and Life Science, National Taiwan University for stereological analysis.

Appendix A. Supplementary data

Supplementary data related to this article can be found at http://dx.doi.org/10.1016/j.neuropharm.2016.02.018.

References

Asahi, S., Egashira, S., Matsuda, M., Iwaasa, H., Kanatani, A., Ohkubo, M., Ihara, M., Morishima, H., 2003. Development of an orexin-2 receptor selective agonist, [Ala(11), D-Leu(15)]orexin-B. Bioorg. Med. Chem. Lett. 13, 111–113.

Azhdari-Zarmehri, H., Reisi, Z., Vaziri, A., Haghparast, A., Shaigani, P., 2013. Involvement of orexin-2 receptors in the ventral tegmental area and nucleus accumbens in the antinociception induced by the lateral hypothalamus stimulation in rats. Peptides 47, 94–98.

Azhdari-Zarmehri, H., Semnanian, S., Fathollahi, Y., 2014. Orexin-A microinjection into the rostral ventromedial medulla causes antinociception on formalin test. Pharmacol. Biochem. Behav. 122, 286–290.

Azhdari Zarmehri, H., Semnanian, S., Fathollahi, Y., Erami, E., Khakpay, R., Azizi, H., Rohampour, K., 2011. Intra-periaqueductal gray matter microinjection of orexin-A decreases formalin-induced nociceptive behaviors in adult male rats. J. Pain 12, 280–287.

Behbehani, M.M., Jiang, M.R., Chandler, S.D., Ennis, M., 1990. The effect of GABA and its antagonists on midbrain periaqueductal gray neurons in the rat. Pain 40, 195–204.

Berkowitz, B.A., 1976. The relationship of pharmacokinetics to pharmacological activity: morphine, methadone and naloxone. Clin. Pharmacokinet. 1, 219–230.

Bingham, S., Davey, P.T., Babbs, A.J., Irving, E.A., Sammons, M.J., Wyles, M., Jeffrey, P., Cutler, L., Riba, I., Johns, A., Porter, R.A., Upton, N., Hunter, A.J., Parsons, A.A., 2001. Orexin-A, an hypothalamic peptide with analgesic properties. Pain 92, 81–90.

Bradford, M.M., 1976. A rapid and sensitive method for the quantitation of microgram quantities of protein utilizing the principle of protein-dye binding. Anal. Biochem. 72, 248–254.
Chang, H., Saito, T., Ohiwa, N., Tateoka, M., Deocaris, C.C., Fujikawa, T., Soya, H., 2007. Inhibitory effects of an orexin-2 receptor antagonist on orexin A- and stress-induced ACTH responses in conscious rats. Neurosci. Res. 57, 462–466.
Cheng, J.K., Chou, R.C., Hwang, L.L., Chiou, L.C., 2003. Antiallodynic effects of intrathecal orexins in a rat model of postoperative pain. J. Pharmacol. Exp. Ther. 307, 1065–1071.
Chiou, L.C., Lee, H.J., Ho, Y.C., Chen, S.P., Liao, Y.Y., Ma, C.H., Fan, P.C., Fuh, J.L., Wang, S.J., 2010. Orexins/hypocretins: pain regulation and cellular actions. Curr. Pharm. Des. 16, 3089–3100.
D'Ambra, T.E., Estep, K.G., Bell, M.R., Eissenstat, M.A., Josef, K.A., Ward, S.J., Haycock, D.A., Baizman, E.R., Casiano, F.M., Beglin, N.C., et al., 1992. Conformationally restrained analogues of pravadoline: nanomolar potent, enantioselective, (aminoalkyl)indole agonists of the cannabinoid receptor. J. Med. Chem. 35, 124–135.
Date, Y., Ueta, Y., Yamashita, H., Yamaguchi, H., Matsukura, S., Kangawa, K., Sakurai, T., Yanagisawa, M., Nakazato, M., 1999. Orexins, orexigenic hypothalamic peptides, interact with autonomic, neuroendocrine and neuroregulatory systems. Proc. Natl. Acad. Sci. U. S. A. 96, 748–753.
de Lecea, L., Kilduff, T.S., Peyron, C., Gao, X., Foye, P.E., Danielson, P.E., Fukuhara, C., Battenberg, E.L., Gautvik, V.T., Bartlett 2nd, F.S., Frankel, W.N., van den Pol, A.N., Bloom, F.E., Gautvik, K.M., Sutcliffe, J.G., 1998. The hypocretins: hypothalamus-specific peptides with neuroexcitatory activity. Proc. Natl. Acad. Sci. U. S. A. 95, 322–327.
Erami, E., Azhdari-Zarmehri, H., Ghasemi-Dashkhasan, E., Esmaeili, M.H., Semnanian, S., 2012. Intra-paragigantocellularis lateralis injection of orexin-A has an antinociceptive effect on hot plate and formalin tests in rat. Brain Res. 1478, 16–23.
Franklin, K.B.J., Paxinos, G., 1997. The Mouse Brain in Stereotaxic Coordinates. Academic Press, San Diego, U. S. A.
Furlong, T.M., Vianna, D.M., Liu, L., Carrive, P., 2009. Hypocretin/orexin contributes to the expression of some but not all forms of stress and arousal. Eur. J. Neurosci. 30, 1603–1614.
Gatley, S.J., Gifford, A.N., Volkow, N.D., Lan, R., Makriyannis, A., 1996. 123I-labeled AM251: a radioiodinated ligand which binds in vivo to mouse brain cannabinoid CB1 receptors. Eur. J. Pharmacol. 307, 331–338.
Gerashchenko, D., Horvath, T.L., Xie, X.S., 2011. Direct inhibition of hypocretin/orexin neurons in the lateral hypothalamus by nociceptin/orphanin FQ blocks stress-induced analgesia in rats. Neuropharmacology 60, 543–549.
Gregg, L.C., Jung, K.M., Spradley, J.M., Nyilas, R., Suplita 2nd, R.L., Zimmer, A., Watanabe, M., Mackie, K., Katona, I., Piomelli, D., Hohmann, A.G., 2012. Activation of type 5 metabotropic glutamate receptors and diacylglycerol lipase-alpha initiates 2-arachidonoylglycerol formation and endocannabinoid-mediated analgesia. J. Neurosci. 32, 9457–9468.
Grisel, J.E., Mogil, J.S., Belknap, J.K., Grandy, D.K., 1996. Orphanin FQ acts as a supraspinal, but not a spinal, anti-opioid peptide. Neuroreport 7, 2125–2129.
Guo, Z.L., Moazzami, A.R., Longhurst, J.C., 2004. Electroacupuncture induces c-Fos expression in the rostral ventrolateral medulla and periaqueductal gray in cats: relation to opioid containing neurons. Brain Res. 1030, 103–115.
Hirose, M., Egashira, S., Goto, Y., Hashihayata, T., Ohtake, N., Iwaasa, H., Hata, M., Fukami, T., Kanatani, A., Yamada, K., 2003. N-acyl 6,7-dimethoxy-1,2,3,4-tetrahydroisoquinoline: the first orexin-2 receptor selective non-peptidic antagonist. Bioorg. Med. Chem. Lett. 13, 4497–4499.
Ho, Y.C., Lee, H.J., Tung, L.W., Liao, Y.Y., Fu, S.Y., Teng, S.F., Liao, H.T., Mackie, K., Chiou, L.C., 2011. Activation of orexin 1 receptors in the periaqueductal gray of male rats leads to antinociception via retrograde endocannabinoid (2-arachidonoylglycerol)-induced disinhibition. J. Neurosci. 31, 14600–14610.
Hohmann, A.G., Suplita, R.L., Bolton, N.M., Neely, M.H., Fegley, D., Mangieri, R., Krey, J.F., Walker, J.M., Holmes, P.V., Crystal, J.D., Duranti, A., Tontini, A., Mor, M., Tarzia, G., Piomelli, D., 2005. An endocannabinoid mechanism for stress-induced analgesia. Nature 435, 1108–1112.
Johnson, P.L., Truitt, W., Fitz, S.D., Minick, P.E., Dietrich, A., Sanghani, S., Traskman-Bendz, L., Goddard, A.W., Brundin, L., Shekhar, A., 2010. A key role for orexin in panic anxiety. Nat. Med. 16, 111–115.
Maione, S., Bisogno, T., de Novellis, V., Palazzo, E., Cristino, L., Valenti, M., Petrosino, S., Guglielmotti, V., Rossi, F., Di Marzo, V., 2006. Elevation of endocannabinoid levels in the ventrolateral periaqueductal grey through inhibition of fatty acid amide hydrolase affects descending nociceptive pathways via both cannabinoid receptor type 1 and transient receptor potential vanilloid type-1 receptors. J. Pharmacol. Exp. Ther. 316, 969–982.
Marcus, J.N., Aschkenasi, C.J., Lee, C.E., Chemelli, R.M., Saper, C.B., Yanagisawa, M., Elmquist, J.K., 2001. Differential expression of orexin receptors 1 and 2 in the rat brain. J. Comp. Neurol. 435, 6–25.
Mobarakeh, J.I., Takahashi, K., Sakurada, S., Nishino, S., Watanabe, H., Kato, M., Yanai, K., 2005. Enhanced antinociception by intracerebroventricularly and intrathecally-administered orexin A and B (hypocretin-1 and -2) in mice. Peptides 26, 767–777.
Mohammad-Pour Kargar, H., Azizi, H., Mirnajafi-Zadeh, J., Ali Reza, M., Semnanian, S., 2015. Microinjection of orexin-A into the rat locus coeruleus nucleus induces analgesia via cannabinoid type-1 receptors. Brain Res. 1624, 424–432.
Nunes-de-Souza, R.L., Graeff, F.G., Siegfried, B., 1991. Strain-dependent effects of morphine injected into the periaqueductal gray area of mice. Braz. J. Med. Biol. Res. 24, 291–299.
Paxinos, G., Watson, C., 1998. The Rat Brain in Stereotaxic Coordinates. Academic Press.
Peyron, C., Tighe, D.K., van den Pol, A.N., de Lecea, L., Heller, H.C., Sutcliffe, J.G., Kilduff, T.S., 1998. Neurons containing hypocretin (orexin) project to multiple neuronal systems. J. Neurosci. 18, 9996–10015.
Rachalski, A., Alexandre, C., Bernard, J.F., Saurini, F., Lesch, K.P., Hamon, M., Adrien, J., Fabre, V., 2009. Altered sleep homeostasis after restraint stress in 5-HTT knock-out male mice: a role for hypocretins. J. Neurosci. 29, 15575–15585.
Sadeghi, S., Reisi, Z., Azhdari-Zarmehri, H., Haghparast, A., 2013. Involvement of orexin-1 receptors in the ventral tegmental area and the nucleus accumbens in antinociception induced by lateral hypothalamus stimulation in rats. Pharmacol. Biochem. Behav. 105, 193–198.
Sagar, S.M., Sharp, F.R., Curran, T., 1988. Expression of c-fos protein in brain: metabolic mapping at the cellular level. Science 240, 1328–1331.
Sakamoto, F., Yamada, S., Ueta, Y., 2004. Centrally administered orexin-A activates corticotropin-releasing factor-containing neurons in the hypothalamic paraventricular nucleus and central amygdaloid nucleus of rats: possible involvement of central orexins on stress-activated central CRF neurons. Regul. Pept. 118, 183–191.
Sakurai, T., Amemiya, A., Ishii, M., Matsuzaki, I., Chemelli, R.M., Tanaka, H., Williams, S.C., Richardson, J.A., Kozlowski, G.P., Wilson, S., Arch, J.R., Buckingham, R.E., Haynes, A.C., Carr, S.A., Annan, R.S., McNulty, D.E., Liu, W.S., Terrett, J.A., Elshourbagy, N.A., Bergsma, D.J., Yanagisawa, M., 1998. Orexins and orexin receptors: a family of hypothalamic neuropeptides and G protein-coupled receptors that regulate feeding behavior. Cell 92, 573–585.
Smart, D., Sabido-David, C., Brough, S.J., Jewitt, F., Johns, A., Porter, R.A., Jerman, J.C., 2001. SB-334867-A: the first selective orexin-1 receptor antagonist. Br. J. Pharmacol. 132, 1179–1182.
Tsou, K., Brown, S., Sanudo-Pena, M.C., Mackie, K., Walker, J.M., 1998. Immunohistochemical distribution of cannabinoid CB1 receptors in the rat central nervous system. Neuroscience 83, 393–411.
Tsujino, N., Sakurai, T., 2009. Orexin/Hypocretin: a neuropeptide at the interface of sleep, energy homeostasis, and reward system. Pharmacol. Rev. 61, 162–176.
van den Pol, A.N., 1999. Hypothalamic hypocretin (orexin): robust innervation of the spinal cord. J. Neurosci. 19, 3171–3182.
Walker, J.M., Huang, S.M., Strangman, N.M., Tsou, K., Sanudo-Pena, M.C., 1999. Pain modulation by release of the endogenous cannabinoid anandamide. Proc. Natl. Acad. Sci. U. S. A. 96, 12198–12203.
Watanabe, S., Kuwaki, T., Yanagisawa, M., Fukuda, Y., Shimoyama, M., 2005. Persistent pain and stress activate pain-inhibitory orexin pathways. Neuroreport 16, 5–8.
Webb, I.C., Patton, D.F., Hamson, D.K., Mistlberger, R.E., 2008. Neural correlates of arousal-induced circadian clock resetting: hypocretin/orexin and the intergeniculate leaflet. Eur. J. Neurosci. 27, 828–835.
Xie, X., Wisor, J.P., Hara, J., Crowder, T.L., LeWinter, R., Khroyan, T.V., Yamanaka, A., Diano, S., Horvath, T.L., Sakurai, T., Toll, L., Kilduff, T.S., 2008. Hypocretin/orexin and nociceptin/orphanin FQ coordinately regulate analgesia in a mouse model of stress-induced analgesia. J. Clin. Invest. 118, 2471–2481.
Yaksh, T.L., Yeung, J.C., Rudy, T.A., 1976. Systematic examination in the rat of brain sites sensitive to the direct application of morphine: observation of differential effects within the periaqueductal gray. Brain Res. 114, 83–103.
Zhu, L., Onaka, T., Sakurai, T., Yada, T., 2002. Activation of orexin neurones after noxious but not conditioned fear stimuli in rats. Neuroreport 13, 1351–1353.